BNL 36119

CONF-850159--2

BNL--36119

DE85 009755

BOSON-FERMION SYMMETRIES IN THE W-Pt REGION

D. D. Warner
Brookhaven National Laboratory
Upton, New York 11973

Invited Talk
VIII Symposium on Nuclear Physics
Oaxtepec, Mexico
January 8-10, 1985

BOSON-FERMION SYMMETRIES IN THE W-Pt REGION

D. D. Warner
Brookhaven National Laboratory
Upton, New York 11973

Invited Talk
VIII Symposium on Nuclear Physics
Oaxtepec, Mexico
January 8-10, 1985

BOSON-FERMION SYMMETRIES IN THE W-Pt REGION

D. D. Warner
Brookhaven National Laboratory
Upton, New York 11973
USA

1. INTRODUCTION

The concept of symmetry in the Interacting Boson Model[1] (IBM) description of even-even nuclei has proved to be one of the model's most important elements, not only because of the recognition of the existence of the symmetries themselves, but also because they provide benchmarks in the formulation of a unified description of a broad range of nuclei. The importance of the recently proposed[2] symmetries in odd-even systems can thus be viewed in the same light, and their role in pointing to a simple prescription for the changing collective structure in odd A nuclei throughout a major shell is likely to prove even more essential, given the much greater complexity of the boson-fermion (IBFM) Hamiltonian[3].

The group structure of a boson-fermion system is described by $U^B(6) \times U^F(m)$ where m specifies the number of states available to the odd fermion, and thus depends on the single particle space assumed. The ability to construct group chains corresponding to the symmetries SU(5), SU(3) or O(6) depends on the value of m, and this problem has already been discussed in detail in a separate contribution[4]. Of the structures studied in detail to date, the case of m=12 is the one with the broadest potential[5]. The fermion is allowed to occupy orbits with j = 1/2, 3/2 and 5/2, so that the assumed single particle space corresponds to the negative parity states available to an odd neutron at the end of the N = 82-126 shell, namely, $p_{1/2}$, $p_{3/2}$ and $f_{5/2}$. The region of interest thus spans the W-Pt nuclei, and since one prerequisite for an odd-A symmetry is the existence of that same symmetry in the neighboring even-even core nucleus, the odd Pt nuclei around A = 196 offer the obvious testing ground for the O(6) limit of U(6/12). The heavier even-even W nuclei, on the other hand, have the characteristics of an axial rotor, and hence the negative parity structure of the neighboring odd W isotopes offers the possibility to study the validity of the SU(3) limit. Finally, given a definition and understanding of these two limits, the construction of a simple description of the transitional odd-A Os nuclei can be considered.

In considering a unified description of the odd-A collective structure in this region, the principal advantage of the IBFM is its inclusion of a core description which can run the full gamut of vibrational, rotational or asymmetric structure, and which incorporates essentially all collective excitations. Thus, in the region of well deformed nuclei, such as W, one can expect the model to

generate an equally detailed description of both the low lying rotational structure which emerges from a Nilsson model treatment, and the subsequent vibrational modes which to date have, in general, been treated only qualitatively. In regions outside those of axially symmetric deformation, such as the heavier Os and Pt nuclei, the IBFM's capabilities should prove even more crucial, since here deficiencies in the core description can manifest themselves even at low excitation energies.

2. ^{195}Pt: THE O(6) LIMIT OF U(6/12)

As pointed out in Section 1, the well established O(6) symmetry in ^{196}Pt and its neighbors[6], coupled with the isolated $p_{1/2}$, $p_{3/2}$ and $f_{5/2}$ orbits available to an odd neutron in this region, implies that the odd Pt nuclei should offer the best opportunity to test the predictions of the O(6) group chain of U(6/12). The results of recent (n,γ) studies[7] of ^{195}Pt have led to a comprehensive level scheme which is compared with the U(6/12) O(6) symmetry in fig. 1. The origins of the theoretical scheme, and its associated quantum numbers, have been discussed in detail elsewhere[8]. It is therefore sufficient to remark here that it offers an adequate description of the observed structure, at least below 600 keV. It is particularly encouraging that a one-to-one correspondence can be made between experimental and theoretical levels up to this energy. Moreover, subsequent (n,n',γ) studies[9] have removed a number of the ambiguities in the empirical spin assignments of fig. 1, and in all cases, the results confirm the association of states shown. Data from single particle transfer studies[10] are also largely in agreement with the symmetry predictions, although some important discrepancies have been found[11] for the reaction ^{195}Pt+^{196}Pt. However, it is possible, and indeed likely, that these stem from uncertainties in the form of the IBFM transfer operator itself. Recent data has also been obtained[12] on B(E2) values in ^{195}Pt and again, these confirm the selection rules mandated by the symmetry scheme. There is evidence of symmetry breaking, at the level of 20-30%, but there is also some indication that this may be largely accounted for by a suitable choice of the relative signs and magnitudes of the boson and fermion effective charges in the E2 operator.

A distinctive feature of the symmetry scheme is the existence of couplets of levels with J, J+1 separated by a constant J(J+1) spacing. This feature shows up clearly in the data and results from the pseudo-spin symmetry inherent in all the group chains of U(6/12). There is, however, a clear discrepancy between theory and experiment at higher excitation energies in that the predicted states in the representation labelled [N,1] are too compressed, relative to the data. A modification to the original scheme which removes this problem, while maintaining the symmetry, is discussed in ref. 13.

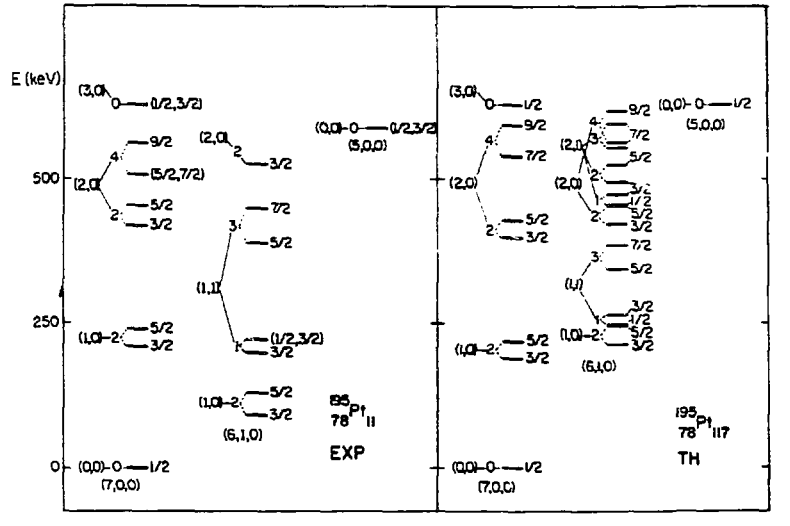

Fig. 1. A comparison of the O(6) symmetry scheme of U(6/12) with the levels of ^{195}Pt.

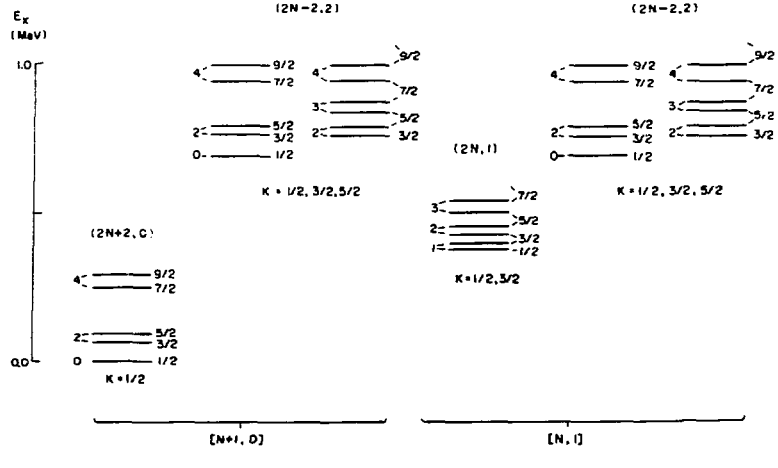

Fig. 2. The SU(3) scheme of U(6/12). Representations are labelled by the (λ,μ) quantum number of $SU^{BF}(3)$ and by the $[N_1N_2]$ labels of $U^{BF}(6)$.

3. THE SU(3) LIMIT OF U(6/12) AND THE NILSSON MODEL

The SU(3) limit of U(6/12) requires a rotational core structure, coupled to j = 1/2, 3/2 and 5/2 orbits. The odd W nuclei represent the best chance of observing characteristics of this symmetry since, in nuclei of lower mass in the well deformed rare earth region, the Fermi surface is progressively farther from the single particle orbits of interest. The structure of the SU(3) level scheme is illustrated in fig. 2 and is defined by the group chain decomposition.

$$U^B(6) \times U^F(12) \supset \boxed{U^B(6) \times U^F(6) \times SU^F(2)}$$

$$\supset U^{BF}(6) \times SU^F(2) \supset SU^{BF}(3) \times SU^F(2) \qquad (1)$$

$$\supset O^{BF}(3) \times SU^F(2) \supset \text{Spin (3)}$$

The corresponding Hamiltonian which describes excitation energies is constructed from the Casimir operators of the groups $U^{BF}(6)$, $SU^{BF}(3)$, $O^{BF}(3)$, and Spin(3). The states thus group into the various (λ,μ) representations of $SU^{BF}(3)$, and within each representation, the equivalent of one or more odd-A rotational bands can be assigned, and are labelled by their appropriate K values. The $SU^{BF}(3)$ representations themselves fall into one of two possible representations of the group $U^{BF}(6)$ which are distinguished by the quantum numbers [N+1,0] and [N,1]. In fact, it will be seen presently that it is the K=1/2 and 3/2 bands of the (2N,1) representation of fig. 2 which form the ground state structure in ^{185}W and this situation can be realized in the symmetry scheme by a suitable adjustment of the relative sizes of the contributions from the Casimir operators of $U^{BF}(6)$ and $SU^{BF}(3)$ in the Hamiltonian.

The SU(3) limit has the attractive advantage that its predictions can be compared with those of the Nilsson model for the same shell model states, so that a more physical interpretation of its structure can be formulated. A comparison of the essential ingredients and approach in each framework is given schematically in fig. 3. The relative energies of the spherical single particle states shown for the U(6/12) system stem from the pseudo L decomposition[14], represented by the boxed portion of the chain decomposition in eq. (1), which treats the fermions as a one-boson system coupled to pseudo spin ±1/2. In the Nilsson scheme, the spherical ordering is different and would remain so if the input energies in the IBFM scheme are taken as quasiparticle energies, since the Fermi surface in the spherical scheme would be expected to be near the $p_{3/2}$ orbit. The core basis in the Nilsson scheme involves only the ground state rotational band, and this is also true for the lowest two representations of the U(6/12) scheme[15]. (The spin cutoff should not

affect the low spin states considered here.) In the Nilsson treatment, the spherical states are first mixed via a quadrupole interaction to generate the Nilsson orbits shown on the right. Note that the solid lines denote orbits stemming from the $p_{1/2}$, $p_{3/2}$ or $f_{5/2}$ shell model states while the dashed Nilsson states originate in the $f_{7/2}$ and $h_{9/2}$ orbits and are therefore outside the U(6/12) basis of interest here. The core states are then effectively coupled

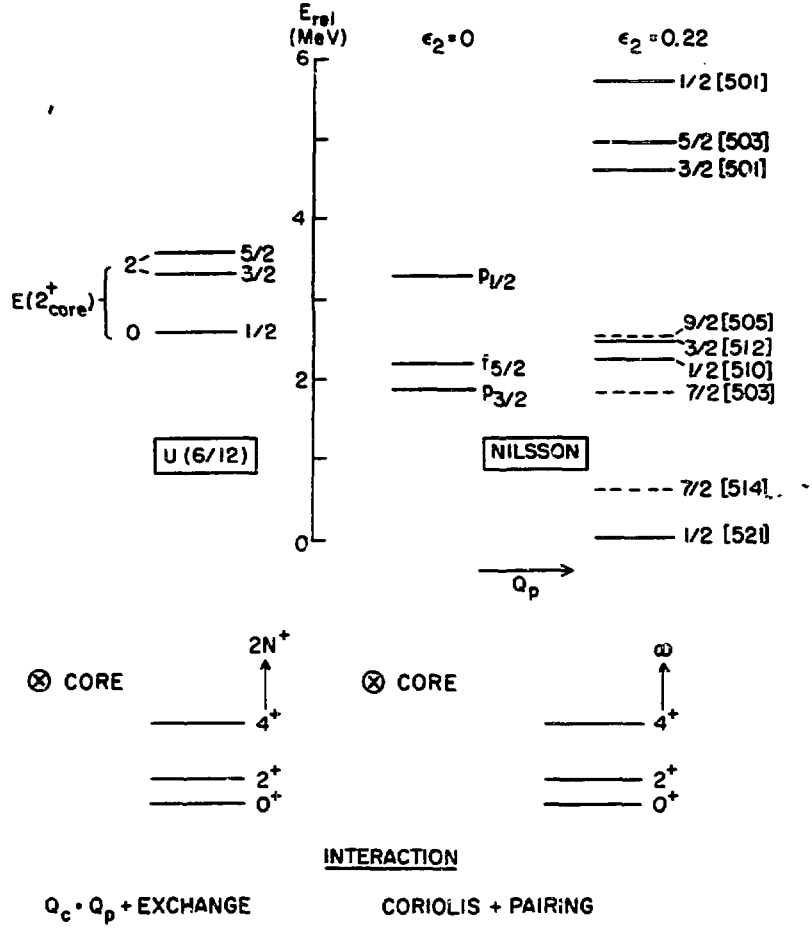

Fig. 3. Schematic indication of the single particle energies and basic approach adopted in the U(6/12) and Nilsson schemes. (See text for further discussion.)

via the introduction of the rotational motion, and the residual Coriolis and pairing interactions are also included, the latter being considered in the deformed single particle potential. The U(6/12) approach starts from a basis comprising the rotational core states coupled to the spherical single particle states, and then applies an interaction which involves a quadrupole-quadrupole and an exchange term. In this case, therefore, the location of the Fermi surface can only be considered in the spherical limit and it is the exchange term which must account for the effects of the deformed potential on the pairing correlations.

The connection between the two bases can be explored via the single particle structure of the wave functions in each case, as shown below.

Nilsson	U(6/12)-SU(3)
Intrinsic wave function:	Core particle wave function:
$\chi_\Omega = \sum_{j\ell} C_{j\ell} \lvert N\ell j\Omega\rangle$	$\lvert I,K,\alpha\rangle = \sum_{jR} a_{jR} \lvert jR;I\alpha\rangle$
Normalization:	Normalization:
$\sum_{\Omega} C^2_{j\ell} = (2j+1)/2$	$\sum_{I,K} a^2_{jR} = 1$
Coriolis mixing:	
$\sum_i a_i \chi^i_\Omega$	
$C^{eff}_{j\ell} = \sum_i a_i C^i_{j\ell}$	$C^{eff}_{j\ell} = \{(2j+1)/2\}^{1/2} a_{j0}$

In the Nilsson scheme, the single particle structure for each orbit is contained in the intrinsic wave function, χ_Ω, in terms of the spherical amplitudes $C_{j\ell}$. The Coriolis interaction produces a mixing of the pure orbits, represented above by the amplitudes a_i, so that the final structure can be represented by the quantity $C^{eff}_{j\ell}$ on the left. In terms of a core particle basis, as used in the IBFM scheme, the appropriate coupling coefficients are simply the Clebsch-Gordon coefficients $\langle j\Omega R0 \mid I\Omega\rangle$. Since these take the value unity for the case R=0, j=I, the $C_{j\ell}$ coefficients are equivalent to the amplitudes a_{j0} on the right, which represents the coupling of the spherical state with spin j to the 0^+ ground state of the core. The different normalizations then imply the form on the right for the quantity $C^{eff}_{j\ell}$ in the U(6/12) basis. Note that Coriolis effects should be included automatically in this case.

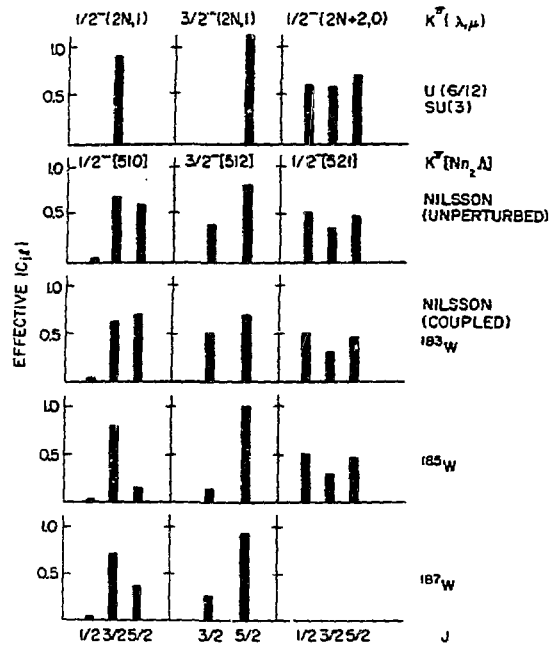

Fig. 4. Values of $C_{j\ell}^{eff}$ in the U(6/12) and Nilsson schemes. Those for the latter are calculated using the wave functions and Coriolis mixing amplitudes of ref. 16.

The amplitudes a_{j0} can be extracted numerically by taking an overlap of the U(6/12) wave functions with those of the appropriate SU(3) core. The resulting values of $C^{eff}_{j\ell}$ for the lowest three SU(3) representations are compared with those for the lowest lying Nilsson bands in fig. 4. At the top of the figure it can be seen that the K=1/2 and 3/2 bands contained in the $(\lambda,\mu) = (2N,1)$ representation have a particularly distinctive structure, which stems from the fact that the amplitudes a_{j0} are identically zero for states with odd values of the pseudo-orbital angular momentum. The corresponding pattern is clearly not observed in the unperturbed Nilsson bands. However, the lower portion of the figure shows the results of earlier Coriolis mixing calculations in the W isotopes[16], and an interesting feature emerges. The mixing between the 1/2[510] and 3/2[512] bands results, in ^{185}W, in a transfer of strength between the 3/2 and 5/2 states which almost exactly cancels one component in each case, producing the structure required for the SU(3) symmetry.

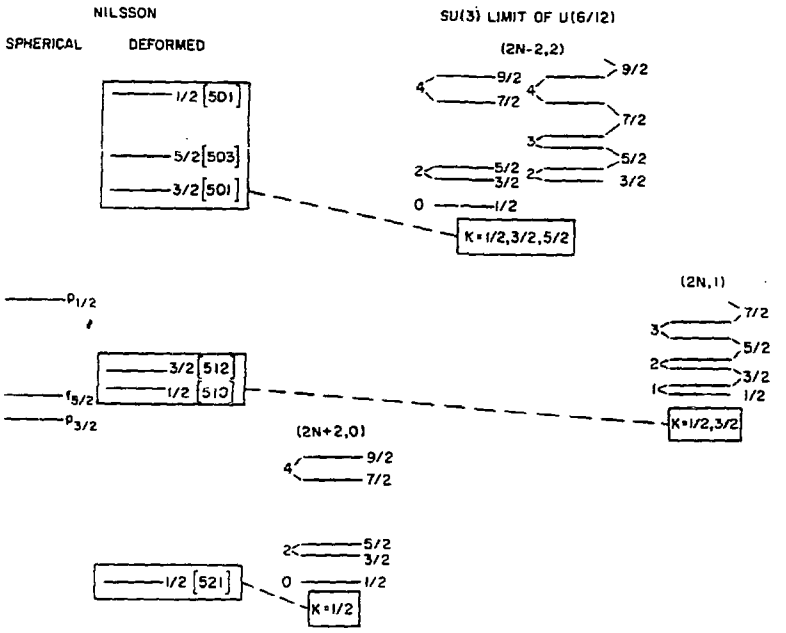

Fig. 5. Relationship between the Nilsson bands from the $p_{1/2}$, $p_{3/2}$, and $f_{5/2}$ spherical states and the U(6/12) SU(3) scheme. The connection for the highest three bands is not exact. (See text and ref. 15 for details.)

A similar analysis[15] can be made between the bands in the (λ,μ) = (2N-2,2) representation, and the remaining Nilsson orbitals of Fig. 3, and the overall results lead to the establishment of an unambiguous correspondence between bands in the two frameworks, which is summarized in fig. 5. However, for the (2N-2,2) representation, the link between the two frameworks is no longer exact, since the IBFM wave functions in this case contain components of the β and γ bands from the core, as well as the ground state band. This results in a predicted fragmentation of the single-particle strength from the corresponding three Nilsson bands. In fact, this fragmentation has been established empirically[17] for some time.

4. APPLICATION TO ^{185}W

It is clear from the preceding discussion that ^{185}W represents the most promising candidate for comparison with the U(6/12) predictions. The Fermi surface is known to lie in the vicinity of the 1/2[510] and 3/2[512] orbits in the W region, and hence the U(6/12) bands in the (2N,1) representations must lie lowest in energy.

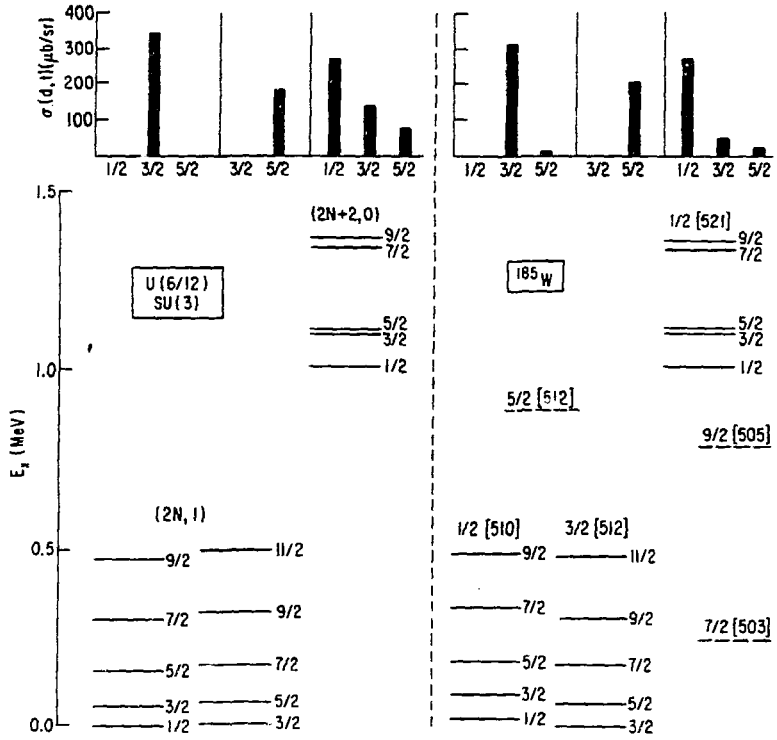

Fig. 6. Predicted and empirical energies and $\sigma(d,t)$ (θ=90°) for assigned Nilsson bands in ^{185}W. Dashed levels denote known bandheads which stem from the $f_{7/2}$ and $h_{9/2}$ shell model states, and are therefore outside the U(6/12) basis. Unassigned states are not included (see text).

Recalling the discussion of Section 2 and fig. 2, the Casimir operator of $U^{BF}(6)$ can bring this representation below the (2N+2,0) states.

The empirical and predicted schemes are compared in fig. 6. There are several important points to note. On the positive side, the same Coriolis mixing which gives rise to the distinctive "fingerprint pattern" of fig. 4 also results in a near degeneracy of states in the lowest lying K=1/2 and 3/2 bands, which appears naturally in the algebraic description. In addition, the distinctive pattern of states in the 1/2[521] band, which in Nilsson terms corresponds to a decoupling parameter close to unity, also emerges naturally from the

symmetry predictions. Both of these features imply that the intrinsic matrix elements $\langle j^- \rangle$ in the Nilsson framework are well reproduced in the alternative scheme. However, it is also evident in fig. 6 that certain observed bands (denoted by dashed lines) cannot be reproduced from the U(6/12) basis because they stem from the $f_{7/2}$ and $h_{9/2}$ shell model states. Moreover, only previously assigned states are shown in the figure. There are additional states observed which have not proved amenable to a Nilsson model description. In order to determine whether some or all of these can be incorporated in the U(6/12) scheme, it is necessary to first obtain information on their number and character, and the results of a recent experiment devoted to this end are currently being studied[18].

A comparison of predicted and empirical (t,t) cross sections is also shown at the top of fig. 6. In the IBFM description of ^{185}W, since the neutron number is past midshell, the number of bosons is equal to that in ^{186}W. Thus the lowest order operator describing the (d,t) reaction can be taken simply as $\zeta_j a^\dagger_j$ where the ζ_j are constants and the matrix elements of $a^\dagger_j$ are equivalent to the quantities $C_{j\ell}^{eff}$ determined earlier. While the results look promising, it must be emphasized that such a simple approach to the single particle transfer problem cannot hope to succeed in the general case in deformed nuclei. Specifically, higher order terms (e.g., $(s^\dagger\tilde{d})a^\dagger_j$) must be included to account for the effect of the non-spherical potential on the pairing correlations. The elucidation of which of the many possible such terms are significant, and their relationship to the underlying microscopy, remains one of the outstanding problems to be solved in the IBFM formalism.

5. THE SU(3)→O(6) TRANSITION AND THE CQF IN ODD A NUCLEI

Despite its limited applicability, it is clear that the U(6/12) SU(3) scheme yields a basically valid description of the low-lying structure of ^{185}W. Thus there are now two benchmarks in the U(6/12) basis, ^{195}Pt and ^{185}W, which define the SU(3) and O(6) limits, respectively, and it is possible to consider a description of the transitional odd A nuclei in between. For the even-even nuclei in this region, a simple approach involves the Consistent Q Formalism (CQF)[19], in which the Hamiltonian is defined by

$$H = -\kappa Q_B \cdot Q_B - \kappa' L \cdot L \qquad (2)$$

where the boson quadrupole operator, Q_B, is

$$Q_B = (s^\dagger\tilde{d} + d^\dagger s)^{(2)} + (\chi/\sqrt{5})\,(d^\dagger\tilde{d})^{(2)}. \qquad (3)$$

The E2 operator is then constrained to take the same form as Q_B. For a given boson number N, the parameter χ alone determines the structure of the wave functions and can be varied in the range defined by the values which generate the SU(3) and O(6) limits,

namely, $-\sqrt{35}/2$ to 0. The advantages of this approach lie chiefly in its simplicity. It involves at least one less parameter than the conventional approach, since the symmetry breaking mechanism is now represented by χ, rather than an extra term in H, but the freedom to vary the structure of the E2 operator is removed. In addition, since the wave functions and E2 operator are uniquely specified by χ (and N), relative B(E2) values and energies depend only on these two parameters. There is also a degree of simplicity gained at the intuitive, or interpretive, level since the changes in structure which result from a change in the equilibrium nuclear shape are now ascribed simply to changes in the form of the quadrupole operator and can, in fact, be simply related[20] to the geometrical β and γ deformation variables.

In order to formulate an equivalent approach for the boson-fermion Hamiltonian it is clearly necessary to develop a compatible parameterization for the fermion degrees of freedom. Referring again to the boxed portion of chain (1) the pseudo-orbital angular momentum decomposition[14] of the fermion space constitutes the crucial feature. This technique corresponds to treating the fermion angular momenta as arising from the coupling of a pseudo L quantum number with L=0 or 2 to a pseudo spin of 1/2.

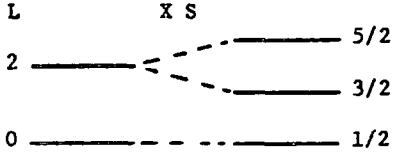

The analogy with the s,d boson space is immediately obvious, and allows a fermion quadrupole operator Q_F to be defined in an equivalent way to Q_B (eq. 2).

$$Q_F = G_F^{(2)}(0,2) + G_F^{(2)}(2,0) + (\chi/\sqrt{5})\ G_F^{(2)}(2,2) \qquad (4)$$

The fermion generators $G_F^{(2)}(\ell,\ell')$ are given in detail elsewhere[8,21]. They simply consist of appropriate combinations of the fermion annihilation and creation operators, such that $G_F^{(2)}(0,2)$ or $G_F^{(2)}(2,0)$ involve couplings of the type $(j,j') = (1/2,3/2)$, $(1/2,5/2)$, while $G_F^{(2)}(2,2)$ involves $(j,j') = (3/2,3/2)$, $(5/2,5/2)$ and $(3/2,5/2)$. The CQF for odd-A nuclei can now be defined by demanding that χ take identical values in Q_B and Q_F.

In the IBFM Hamiltonian which corresponds to the SU(3) group chain (1) the quadratic Casimir operator of the group $SU^{BF}(3)$ generates a quadrupole interaction of the form

$$Q \cdot Q = (Q_B + Q_F) \cdot (Q_B + Q_F) \tag{6}$$

where Q_B and Q_F are defined by eqs. 3 and 4 with $\chi = -\sqrt{35}/2$. It is then easy to show that when $\chi=0$, the Q·Q interaction reduces to the form

$$C_{20^{BF}(6)} - C_{20^{BF}(5)} \tag{7}$$

which are the Casimir operators required in place of that of $SU^{BF}(3)$ to produce the O(6) limit of U(6/12). However, as in the even-even case, the O(6) limit produced in this way is not the most general one, in that the O(6) and O(5) contributions are constrained to be equal. The first success of this approach, therefore, can be found by considering the magnitudes of these terms found in an earlier fit[21] to the nucleus ^{195}Pt which, by virtue of its core nucleus ^{196}Pt, is the obvious odd-A candidate to exhibit this symmetry. In this previous calculation, no restriction was placed on the relative sizes of the two terms but, in fact, the fit yielded 33.5 and 35.0 keV for the coefficients of the O(6) and O(5) terms, respectively.

In a transitional situation, where χ takes a value intermediate between $-\sqrt{35}/2$ and 0, the contributions to the Hamiltonian from the Casimir operators of $U^{BF}(6)$, $O^{BF}(3)$ and Spin (3) remain diagonal, so that the symmetry breaking mechanism is contained only within the Q·Q term, and hence is uniquely specified by χ. Thus, just as in the even-even case, the wave functions depend only on χ, and the boson number N. Also, if the E2 operator is defined as

$$T(E2) = \alpha\ (Q_B + Q_F)$$

then all relative B(E2) values are likewise uniquely determined. Thus, a situation totally analogous to that in the case of the even-even CQF is obtained, in that the behavior of relative energies, B(E2)'s and in this instance, single particle structure factors, can be predicted across the transition from deformed to γ-unstable structure.

6. CHARACTERISTICS OF THE SU(3)-O(6) TRANSITION

The correct empirical ordering of representations for ^{185}W is illustrated in fig. 7a. An additional label has also been introduced in this figure, which proves useful in tracking the behavior of the SU(3) states through the transition to O(6) structure. It is evident in fig. 7a that the pseudo-L values given on the left of the levels themselves group into rotational band structures, which can be distinguished by means of a pseudo-projection quantum number K_p, as shown. The behavior of the states within each pseudo-K band as $\chi \to 0$

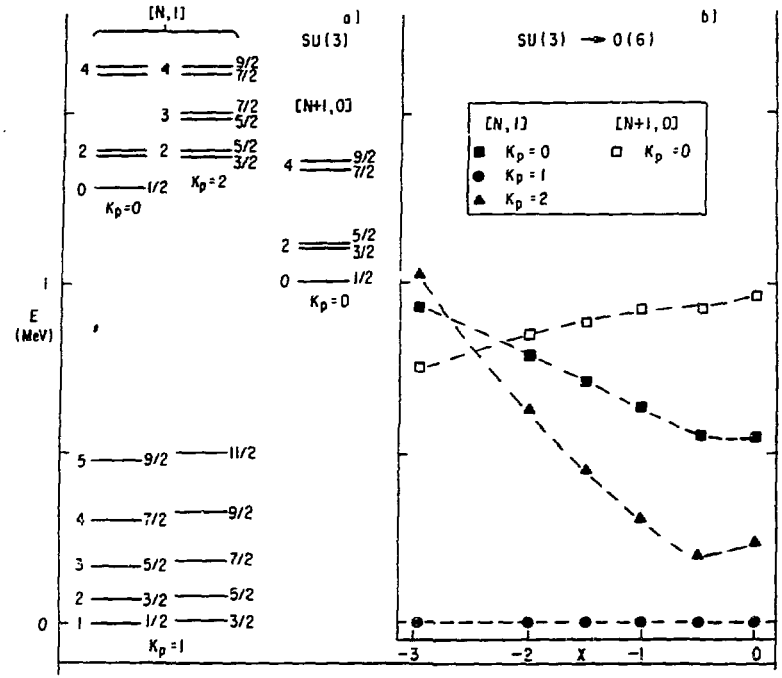

Fig. 7. (a) The SU(3) limit. Bands have been labelled by the pseudo-projection quantum number K_p. (b) Schematic indication of the evolution of the bands as χ changes from its SU(3) value (-2.958) to O(6) (0).

is then displayed in fig. 7b, the boson number and all other coefficients being kept constant. This figure is necessarily schematic, since the rotational band structure is eventually lost as the O(6) limit is approached. Nevertheless, the most important features are evident, namely, that the K_p=1 states remain lowest in energy while the most significant change is the rapid descent of the K_p=2 states, which eventually mix strongly with the ground state structure around χ = -0.5.

The empirical situation is depicted in fig. 8. At the top of this figure, the "benchmark" SU(3) and O(6) structures of ^{185}W and ^{195}Pt are shown. The transitional region of interest spans the odd Os nuclei, and throughout these isotopes, the low lying structure mimics that of ^{185}W, as evident in the bottom half. The first four low spin states are those originating from the near-degenerate K=1/2 and K=3/2 bands, and the single particle strength resides in the first 5/2 and second 3/2 states in all cases. Moreover, the ratio of

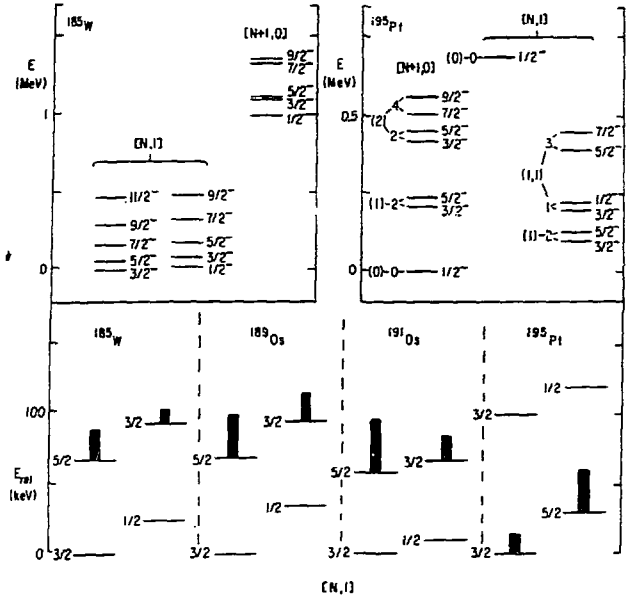

Fig. 8. (Top) The characteristic SU(3) and O(6) structure in ^{185}W, ^{195}Pt and (Bottom) the (d,t) single particle structure factors across the region in the low lying group of states shown (see text for details). Data are from refs. 7, 16, 22, and 23.

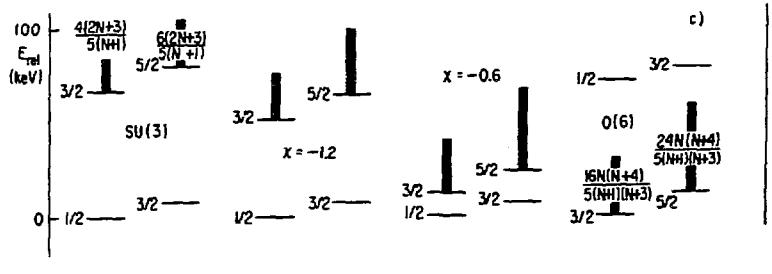

Fig. 9. Predicted changes in the (d,t) structure factors for the lowest lying states. From the schematic calculation of fig. 7b.

the 5/2 and 3/2 strength in each case remains rather constant. However, while these strengths can be reasonably well described in ^{185}W in terms of the appropriate Coriolis-mixed Nilsson orbits, their magnitudes grow in the odd Os nuclei, to the extent that they can no longer be accounted for in a simple Nilsson framework[22,23]. Of course, such problems are hardly surprising in this region given that the neighboring even-even nuclei no longer exhibit the characteristics of axially symmetric rotors.

In ^{195}Pt, the situation changes in two important respects. Firstly, the analogues of the four lowest states in the W and Os nuclei, which are characterized by $U^{BF}(6)$ quantum numbers [N,1] in fig. 7, no longer form the ground state structure, but appear slightly higher in energy, as is evident in the upper portion of fig. 8. In addition, the order of the 3/2, 5/2 and 1/2, 3/2 couplets is reversed. The single particle structure factors, however, still follow the pattern established in the W, Os nuclei. The calculated structure of the low lying states across the transition region is shown in fig. 9. It is clear that the most important empirical features of the transitions emerge naturally from this description. The single particle structure factors are in fact predicted to maintain a constant ratio, S(5/2):S(3/2) = 3:2, independent of χ, while the absolute magnitudes grow as $\chi \to 0$. Moreover, the reversal in the ordering of the two pseudo-spin couplets is also reproduced. Finally, it should be noted that only χ has been varied to produce fig. 9. Details concerning the ordering and correct energies of states can be improved by variation of the remaining diagonal terms in the Hamiltonian. In particular, the correct positioning of the states of fig. 9 in the case of ^{195}Pt requires an adjustment of the $U^{BF}(6)$ contribution.

In the preceding discussion of the structure factors of the low lying states, the lowest order transfer operator of the form $\zeta_j a^+_j$ has been assumed to describe the (d,t) reaction in this region, with $\zeta_{3/2} = \zeta_{5/2}$. More generally, with this operator, the ratio of structure factors for any two states with the same spin will depend only on χ and N. An example is shown in fig. 10, where the ratio for the $3/2_2$ state in the K_p=1 band, and the $3/2_1$ state in the K_p=2 band is plotted. However, another feature of this Hamiltonian is that the squares of the matrix elements of $a^+_{5/2}$ and $a^+_{3/2}$ are always in the ratio 3:2 for two members of a pseudo spin couplet with L=2. As pointed out already in the context of fig. 9, this ratio is constant for all χ values. Thus the curve of fig. 10 applies equally to the ratio of structure factors from the accompanying L=2 5/2 states in each case. The curve has been drawn for N=9, which is appropriate to ^{189}Os, and in that case, the experimental values are R(3/2) = 0.43(6) and R(5/2) = 0.48(7), and hence consistent with equality. The range corresponding to their mean value and error is drawn on the figure, and defines a range of χ values for ^{189}Os, centered on $\chi = -1.5$.

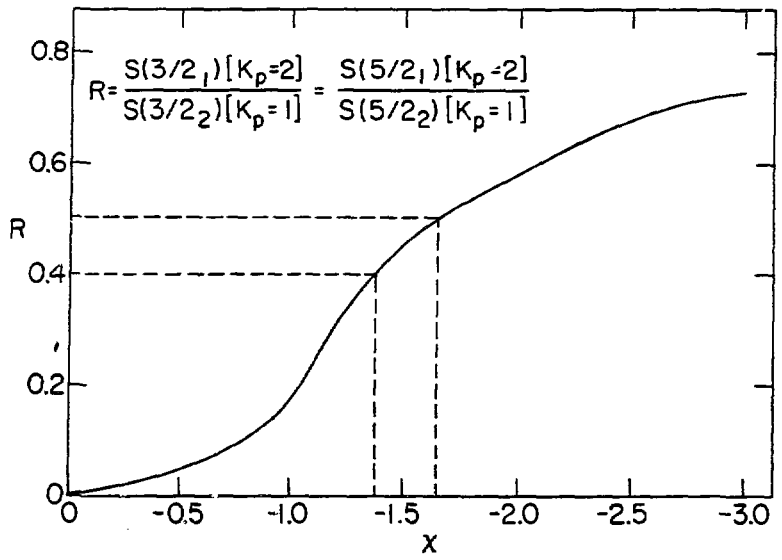

Fig. 10. Predicted ratio of indicated (d,t) structure factors as a function of χ, for N=9. The dashed lines correspond to the mean of the two empirical ratios for ^{189}Os.

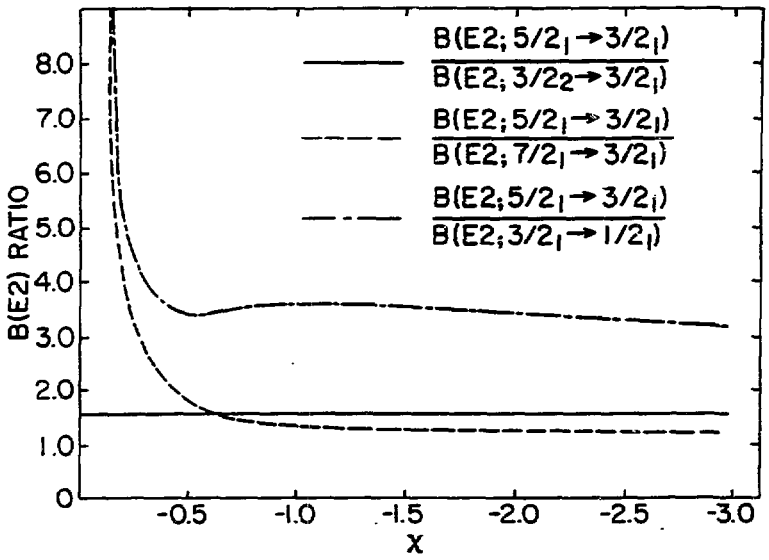

Fig. 11. Predicted B(E2) ratios vs. χ for N=9.

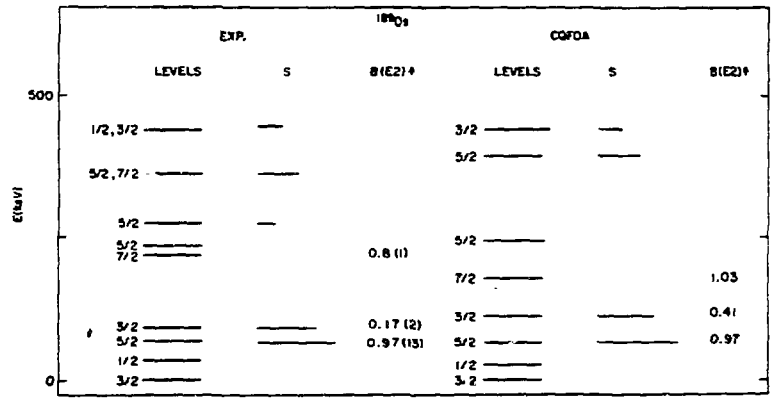

Fig. 12. Calculated and empirical negative-parity structure in ^{189}Os. Lines under S give the relative magnitudes of the (d,t) structure factors. B(E2)↑ implies B(E2) value from the ground state in e^2b^2.

Similar types of predictions can be made for B(E2) values, again couched in terms of ratios to avoid the necessity to specify the effective charge. Some examples are shown in fig. 11, again for N=9, for the lowest lying states. Here, the transition to O(6)-like structure around $\chi = -0.5$ is particularly evident. Also, one ratio maintains a constant value throughout, and this feature again arises from the fact that the pseudo-L symmetry is conserved.

To conclude, the results of figs. 10 and 11 can be combined and compared with the low lying structure in ^{189}Os, as shown in fig. 12. Note that in the experimental part of this figure, the low lying $9/2^-$ and $7/2^-$ states which are known[22] to originate from the $h_{9/2}$ shell model orbit are omitted, since they lie outside the U(6/12) basis being considered here. However, there is very little mixing between these states and the j=1/2, 3/2, 5/2 orbits, so that their neglect should not significantly affect the comparison with the remaining levels.

The agreement for the (d,t) structure factors is excellent, the data reflecting both the 3:2 ratio for each 5/2-3/2 couplet, as well as the predicted absolute magnitudes. The three strongest predicted B(E2) strengths from the ground state are also shown, and these coincide with the strongest measured values[24]. However, in this case, there is a discrepancy of a factor of two for the $3/2_2$ state. The other apparent discrepancy is the existence of an additional $5/2^-$ state in the empirical level scheme, which cannot be accounted for by the theory. This could originate from a coupling between the low-lying $h_{9/2}$ bandhead and the quasi-γ band, and hence lie outside the

U(6/12) basis. However, it should be recognized that there is still some uncertainty concerning the spin assignment of this and many other low-lying states in the odd-Os nuclei, and there is also no guarantee that all low-spin excitations have been identified. A series of (n,γ) studies have therefore been initiated at Brookhaven National Laboratory to clarify the empirical situation in this region.

ACKNOWLEDGEMENTS

The work reported here is the result of a number of collaborations, and the reader is directed to the original references cited in the text for a list of all participants. Particular thanks are due to A. M. Bruce, P. van Isacker and J. Jolie in connection with the studies of ^{185}W and the extension of the CQF to odd A nuclei; also to R. Bijker for numerous discussions concerning the link between the general IBFM Hamiltonian and the symmetries; and to R. F. Casten in the case of the odd Pt studies.

Research has been performed under contract DE-AC02-76CH00016 with the United States Department of Energy.

REFERENCES

1. A. Arima and F. Iachello, Ann. Phys. (N.Y.) 99, 253 (1976); 111, 201 (1978); 123, 468 (1979).
2. F. Iachello, Phys. Rev. Lett. 44, 772 (1980).
3. F. Iachello and O. Scholten, Phys. Rev. Lett. 43, 679 (1979).
4. A. Frank, contribution to these proceedings.
5. A. B. Balentekin, I. Bars, R. Bijker, and F. Iachello, Phys. Rev. C27, 1761 (1983).
6. R. F. Casten and J. A. Cizewski, Nucl. Phys. A309, 477 (1978).
7. D. D. Warner, R. F. Casten, M. L. Stelts, H. G. Borner, and G. Barreau, Phys. Rev. C26, 1921 (1982).
8. P. Van Isacker, A. Frank and H. Z. Sun, Ann. Phys. (N.Y.) 157, 183 (1984), and R. Bijker and F. Iachello, Ann. Phys. (N.Y.), in press.
9. A. P. Ghatak-Roy and S. W. Yates, Phys. Rev. C28, 2521 (1983).
10. M. Vergnes, G. Berrier-Ronsin, and R. Bijker, Phys. Rev. C28, 360 (1983).
11. M. Vergnes, G. Berrier-Ronsin, G. Rotbard, J. Vernotte, J. M. Maison, and R. Bijker, Phys. Rev. C30, 517 (1984).
12. A. M. Bruce, W. Gelletly, W. R. Phillips, J. Lukasiak, and D. D. Warner, Bull. Am. Phys. Soc. 29, 1049 (1984), and to be published.
13. M. Vallieres, H. Z. Sun, D. H. Feng, R. Gilmore, and R. F. Casten, Phys. Lett. 135B, 339 (1984).
14. K. T. Hecht and A. Adler, Nucl. Phys. A137, 129 (1969); A. Arima, M. Harvey and K. Shimizu, Phys. Lett. 30B, 517 (1969); J. N. Ginnochio, Ann. Phys. (N.Y.) 126, 234 (1980).
15. D. D. Warner, Phys. Rev. Lett. 52, 259 (1984) and D. D. Warner and A. M. Bruce, Phys. Rev. C30, 1066 (1984).

16. R. F. Casten, P. Kleinheinz, P. T. Daly, and B. Elbek, Mat. Fys. Medd. Dan. Vid. Selsk 38, No. 13 (1972).
17. R. F. Casten, D. D. Warner, and J. A. Cizewski, Nucl. Phys. A333, 237 (1980).
18. A. M. Bruce and D. D. Warner, to be published.
19. D. D. Warner and R. F. Casten, Phys. Rev. Lett. 48, 1385 (1982); Phys. Rev. C28, 1728 (1983).
20. J. N. Ginocchio and M. W. Kirson, Nucl. Phys. A350, 31 (1980).
21. R. Bijker, Ph.D. Thesis, University of Groningen, 1984.
22. D. Benson, P. Kleinheinz and R. K. Sheline, Phys. Rev. C14, 2095 (1976).
23. D. Benson, P. Kleinheinz, R. K. Sheline, and E. B. Shera, Z. Physik A281, 145 (1977).
24. R. B. Firestone, Nucl. Data Sheets 34, 537 (1981).